

Studying the Intracellular Dissociation of Polymer–Oligonucleotide Complexes by Dual Color Fluorescence Fluctuation Spectroscopy and Confocal Imaging[†]

B. Lucas, K. Remaut, N. N. Sanders, K. Braeckmans, S. C. De Smedt,* and J. Demeester

Laboratory of General Biochemistry and Physical Pharmacy, Ghent University, Harelbekestraat 72, 9000 Ghent, Belgium

Received October 29, 2004; Revised Manuscript Received April 6, 2005

ABSTRACT: To transfect cells, cationic polymers as well as cationic liposomes are widely investigated as carriers for both oligonucleotides and plasmid DNA. A major step in the successful intracellular delivery of the DNA is the release from its carrier. In this study, dual color fluorescence fluctuation spectroscopy (dual color FFS) was explored in order to characterize the intracellular dissociation of cationic polymer/oligonucleotide complexes. As a model, rhodamine green-labeled oligonucleotides (RhGr-ONs) were complexed with Cy5-labeled polymers of either high molar mass (Cy5-graft-pDMAEMA, 1700 kDa) or low molar mass [Cy5-poly(L-lysine), Cy5-pLL, 30 kDa]. The FFS results were compared with confocal laser scanning microscopy (CLSM) observations. CLSM proved that Cy5-graft-pDMAEMA/RhGr-ON complexes endocytosed by Vero cells dissociate in the cytoplasm: the polymer was only detected in the cytoplasm whereas the (released) RhGr-ONs accumulated in the nucleus. Transfecting Vero cells with Cy5-pLL/RhGr-ON complexes resulted, however, in colocalization of polymer and oligonucleotides in the nucleus. In the latter case, CLSM was not able to prove whether intact Cy5-pLL/RhGr-ON complexes were present in the nucleus or whether both components were located together in the nucleus without being associated. Dual color FFS, which monitors the movement of (dual labeled) fluorescent molecules, was able to answer this question. As a Cy5-pLL/RhGr-ON complex is multimolecular, i.e., it consists of many RhGr-ONs associated with many Cy5-pLL chains, it is both highly green and red fluorescent. Consequently, when Cy5-pLL/RhGr-ON complexes move through the excitation volume, the (green and red) detectors of the FFS instrument detect simultaneously a strong green and red fluorescence peak. Upon transfecting the Vero cells with Cy5-pLL/RhGr-ON complexes, FFS was indeed able to detect simultaneously green and red fluorescence peaks in the cytoplasm but never in the nucleus. From these results we conclude that the Cy5-pLL and RhGr-ONs present in the nucleus after transfection were not associated.

Since more than a decade, antisense oligonucleotides (ONs)¹ were investigated for the selective inhibition of various genes (1). More recently, double-stranded RNA was found to initiate sequence-specific gene silencing in mammalian cells (2–4). Over 20 antisense candidates are currently in various stages of clinical development, whereas second and third generation (backbone modified) ONs promise a lower toxicity and an increased stability against enzymatic degradation (5). Several laboratories have been encouraged to look for appropriate pharmaceutical carrier systems for ONs, as their cellular delivery is limited. Different types of cationic lipids and cationic polymers are

under investigation to solve problems of hydrophilicity, size, negatively charged backbone, and nuclease sensitivity (6, 7). Cationic lipids as well as cationic polymers spontaneously form soluble interpolyelectrolyte complexes with negatively charged nucleic acids, called lipoplexes and polyplexes, respectively (8). The physicochemical features that govern the biological activity of lipoplexes and polyplexes are, however, not well understood, partly due to the complexity of the association and dissociation behavior of such complexes. Indeed, a critical step in the delivery of ONs is the dissociation of the ONs from the complexes at the right place, i.e., in the cytoplasm of the target cell (9). If the affinity between the ONs and the cationic carriers is too low, the complex will dissociate prematurely (e.g., when it is still in the blood stream or in the extracellular environment), while a strong affinity might prevent the release of the ONs intracellularly. A critical balance between “being associated extracellularly” and “being dissociated intracellularly” needs to be maintained. Although it is out of the scope of this report to review the results obtained in studies on the biophysical behavior of polymer/ON complexes in cells, a brief glance into the literature reveals examples of polyplexes that dissociate in the cytosol, whereas others are believed to enter the nucleus prior to dissociation (10).

[†] IWT-Flanders, Ghent University (UG-BOF), and FWO-Flanders (G.0310.02) supported this project through instrumentation credits and financial support. B.L. is a doctoral fellow of IWT. K.R. is a doctoral fellow of FWO-Flanders. N.N.S. and K.B. are postdoctoral fellows of FWO-Flanders.

* To whom correspondence should be addressed. Tel: 0032-9-2648076. Fax: 0032-9-2648189. E-mail: stefaan.desmedt@ugent.be.

¹ Abbreviations: CLSM, confocal laser scanning microscopy; DMEM, Dulbecco’s modified Eagle’s medium; DS, dextran sulfate; FBS, fetal bovine serum; FFS, fluorescence fluctuation spectroscopy; graft-pDMAEMA, pegylated poly[2-(dimethylamino)ethyl]methacrylate-co-aminoethyl methacrylate; kDa, kilodalton; MWCO, molecular weight cutoff; ON(s), oligonucleotide(s); pEG, poly(ethylene glycol); pLL, poly(L-lysine); RhGr, rhodamine green.

Dual color microscopy has been used frequently to study the intracellular behavior of oligonucleotide/cationic carrier complexes, since it allows the simultaneous observation of the DNA and the cationic carrier in the cell (11–13). A lack of colocalization proves that the DNA is released from its carrier. Colocalization of the fluorescent markers may indicate that the DNA and its carrier are associated. In the latter case, however, it remains possible that the fluorescent labeled molecules are colocalized without being associated. Compared to the spatial analysis of fluorescent labeled molecules, the temporal analysis of the movement of these molecules could be better to conclude whether the fluorescent labeled species are migrating together, i.e., are still associated. Fluorescence fluctuation spectroscopy (FFS), which can be applied on a cellular scale (14), has potential for that purpose. While dual color microscopy answers the question whether the carrier and the oligonucleotides are located together, dual color FFS may answer the question whether they really move together.

Basically, FFS monitors fluorescence intensity fluctuations in the excitation volume of a confocal microscope. The fluorescence fluctuations are due to the diffusion of fluorescent molecules in and out of the excitation volume. In dual color FFS, both interacting components are labeled with spectrally different fluorophores (e.g., red and green), and their emission light is detected separately by two detectors monitoring the *same* excitation volume. When dissociated, the red and green labeled components (which diffuse independently of each other in and out of the excitation volume) are asynchronously detected by the red or green detector. However, when associated, the complex, which diffuses in and out of the excitation volume, is detected in both detectors *simultaneously* because it bears both red and green fluorophores (15).

In our former work, we have proved that *in buffer* the association and dissociation of oligonucleotides to/from cationic polymers can be monitored by FFS (16–20). When associating, the amount of detected free ONs decreases, and highly fluorescent “multimolecular” polymer/ON complexes appear (existing out of many ONs bound to many polymer strands) which are clearly detected by FFS. When dissociating, the amount of free ONs increases, and the multimolecular complexes disappear. To our knowledge, no reports in the literature deal with FFS on polymer/ON complexes in cells. In this study, we wish to explore (1) if dual color FFS is able to detect intact and dissociated polymer/ON complexes in the cytoplasm and in the nucleus of living cells and (2) to what extent does dual color FFS provide additional information to confocal microscopy.

MATERIALS AND METHODS

Oligonucleotides. The 25-mer phosphodiester oligonucleotides (5′-TCT-GGG-TCA-TCT-TTT-CAC-GGT-TGG-C-3′) (molar mass 8 kDa) and the RhGr-labeled analogue were synthesized by Eurogentec (Seraing, Belgium). Each oligonucleotide contained one RhGr label at its 5′ end. The concentration of the ON stock solutions (in phosphate-buffered saline) was determined by absorption measurements at 260 nm (1 OD₂₆₀ = 33 μg of ONs/mL). The contribution of the label to the absorption at 260 nm was taken into account in the determination of the concentration of the

labeled ONs. The ON stock solutions were further diluted with Hepes buffer (20 mM Hepes at pH 7.4).

Polymers and Polystyrene Nanoparticles. Poly(L-lysine) was purchased from Sigma (St. Louis, MO). The viscosimetric average molar mass equaled 30 kDa and was determined by the supplier. Cy5-labeled poly(L-lysine) (Cy5-pLL) was prepared using succinimidyl ester-activated Cy5 dye (Cy5-SE) (FluoroLinkCy5 monofunctional dye; Amersham Pharmacia, Piscataway, NJ), following the manufacturer's procedure. The resulting labeled polymer was purified on a G25 Sephadex column (10 × 100 mm), which was previously equilibrated with Hepes buffer (20 mM, pH 7.4). The fractions containing fluorescent pLL were collected. Finding the amine concentration using the method of Snyder and Sobocinski (21) and measurement of the absorbance of the label allowed the determination of the average number of labels attached to the pLL. It was calculated that, on average, one pLL chain bore one Cy5 label.

Pegylated poly[2-(dimethylamino)ethyl]methacrylate-*co*-aminoethyl methacrylate (pEG-pDMAEMA-*co*-AEMA, molar mass 1700 kDa, 8 mol % AEMA, abbreviated as *graft*-pDMAEMA) was a generous gift of the University of Utrecht. Part of AEMA (maximum 25%) was conjugated with pEG (molar mass 5 kDa), using a versatile method to synthesize pDMAEMA conjugates as described elsewhere (22). Succinimidyl ester-activated Cy5 dye was used to label part of the nonpegylated AEMA groups. The nonconjugated label was removed by means of dialysis (MWCO 12 kDa; Medicell International Ltd.). It could be calculated that each polymer chain bore 12 fluorescent labels. Stock solutions of Cy5-labeled *graft*-pDMAEMA were prepared in Hepes buffer (20 mM Hepes, pH 7.4).

Dextran sulfate (DS) was purchased from Sigma (St. Louis, MO). The molar mass and sulfate content, as provided by the supplier, equaled respectively 500 kDa and 2.3 sulfate groups per glucosyl residue. Stock solutions were prepared in Hepes buffer.

Tetraspeck nanobeads (Molecular Probes, Eugene, OR) of 90 and 500 nm (diameter) were used. The nanobeads contain both red and green fluorophores. Stock solutions were prepared in Hepes buffer. Prior to use, the bead dispersions were sonified for 10 min.

Preparation of Polymer/ON Complexes. The polymer/ON complexes were prepared by adding (in one step) a volume of the cationic polymer solution to an equal volume of the ON solution, followed by vortexing during 10 s. To obtain the final ON concentration of 10 μg/mL (1.2 μM), the dispersions were further diluted. The polyplexes were allowed to equilibrate for 30 min at room temperature prior to use.

The ± charge ratio, i.e., the ratio of the number of positive charges on the polymer chains to the number of negative charges on the ONs, was calculated assuming that 1 μg of 25-mer ONs contained 3.43 nmol of negative charges, that 1 μg of pLL contained 7.81 nmol of positive charges (as calculated from the molar mass of the lysine monomer, the pK_a of lysine, and the pH of the solutions), and that 1 μg of *graft*-pDMAEMA contains 1.99 nmol of positive charges (as calculated from the molar mass and the pK_a of the DMAEMA monomer and the degree of substitution).

Cell Culture. Vero cells (African green monkey kidney cells, ATCC no. CCL-81) were cultured in Dulbecco's

modified Eagle's medium (DMEM) without phenol red (Gibco, Merelbeke, Belgium) containing 2 mM glutamine, 10% fetal bovine serum (FBS), and 1% penicillin–streptomycin. Cells were grown to 70% confluency on glass-bottomed Petri dishes (part no. PG-1.5-14-F, glass bottom no. 1.5; MatTek Corp.) at 37 °C in a humidified atmosphere containing 5% CO₂.

Fluorescence Fluctuation Spectroscopy. In this study FFS experiments were performed on a (dual color) FFS setup installed on a MRC1024 Bio-Rad confocal laser-scanning microscope as described elsewhere (16). The 488 and 647 nm lines of the same KrAr laser were used to respectively excite RhGr and Cy5. To verify whether the excitation and the detection volume optimally overlapped, the system was optimized as described by Schwille et al. (23).

FFS basically monitors fluorescence intensity fluctuations in the excitation volume of a microscope (15, 24). The fluorescence fluctuations are due to the diffusion of fluorescent molecules in and out of the excitation volume. The fluorescence fluctuations thus obtained are further processed by correlation analysis in order to calculate the average diffusion coefficient. Equation 1 describes the autocorrelation function in case only one type of fluorescent species is moving through the excitation volume. Fitting the experimental autocorrelation curve to eq 1 allows calculating the amount of fluorescent molecules in the excitation volume (N) and their average diffusion time (τ_D). From the latter, the average diffusion coefficient can be calculated using the experimental diffusion time of rhodamine dye with the known diffusion coefficient of 2.8×10^{-6} cm²/s.

$$G(t) = \frac{1}{N} \left(\frac{1}{1 + t/\tau_D} \right) \left(\frac{1}{1 + \left(\frac{\omega_1}{\omega_2} \right)^2 (t/\tau_D)} \right)^{1/2} \quad (1)$$

ω_1 and ω_2 represent the radius and half of the height of the excitation volume. The average diffusion time τ_D is related to the diffusion coefficient (D):

$$\frac{\omega_1^2}{4\tau_D} = D \quad (2)$$

In dual color FFS, the interacting components are labeled with spectrally different fluorophores (e.g., red and green), and their emission light is detected separately by two detectors monitoring the *same* excitation volume (15). When dissociated, the components in the excitation volume are detected asynchronously by either the red or green detector, as they carry a red *or* a green fluorophore. However, when associated, the resulting complexes are detected by both detectors *simultaneously* because they bear both red and green fluorophores. Autocorrelation analysis of the fluorescence fluctuations recorded by the green detector describes the diffusion behavior of all molecules emitting green light, regardless of whether they are free or associated with red-labeled components. Autocorrelation analysis of the red detector signal describes the diffusion behavior of all red-labeled molecules.

(A) **FFS Measurements in Buffer.** Cy5-pLL/RhGr-ON dispersions (as described above) were further diluted with Hepes buffer until a final ON concentration of 0.2 μ g/mL (24 nM) is reached. After dilution, 50 μ L of the sample

was immediately transferred into a glass-bottomed 96-well plate (Grainer Bio-one, Frickenhausen, Germany) to begin the FFS measurements. Diffusion coefficients were calculated using the average diffusion time of at least 20 measurements. Each Cy5-pLL/RhGr-ON dispersion was independently prepared three times, and each preparation was measured at least 10 times. The fluorescence fluctuation profiles shown in the figures were representative for the measurements done on the respective Cy5-pLL/RhGr-ON dispersions.

(B) **FFS Measurements in Cells.** FFS measurements were done on Vero cells grown to 70% confluency on glass-bottomed Petri dishes (part no. PG-1.5-14-F, glass bottom no. 1.5; MatTek Corp.).

In the transfection experiments, 150 μ L of polymer/RhGr-ON complexes (0.5 μ M RhGr-ONs, \pm charge ratio of 10) in serum-free DMEM was added to the Vero cells and incubated for 1 h at 37 °C. The cells were subsequently washed with PBS, submerged with imaging medium (DMEM containing serum and 10 mM Hepes), and incubated at 37 °C until examination.

In the microinjection experiments, a Femtojet microinjector and an Injectman NI 2 micromanipulator (Eppendorf) were used. The Vero cells were injected (in the cytoplasm or in the nucleus) with respectively free RhGr-ONs (10 μ M) or Cy5-pLL/RhGr-ONs (10 μ M RhGr-ONs, \pm charge ratio of 20) prepared in Hepes buffer.

FFS measurements were done in randomly selected places in the cytoplasm or nucleus. To ensure measurements in viable cells, only nonrounded cells without the appearance of cytoplasmic blebs were selected. Confocal sections in the z -direction were taken every 0.5 μ m in order to position the excitation volume in the cell. After the CLSM/FFS measurements, cell viability was evaluated using propidium iodide.

RESULTS AND DISCUSSION

FFS on Cy5-pLL/RhGr-ON Complexes in Buffer. The association of RhGr-ONs to Cy5-pLL clearly influences the fluorescence fluctuation profiles as measured by both detectors. Highly fluorescence peaks appear in the red and green detector, which we term respectively “Cy5 peaks” and “RhGr peaks”. It is especially clear that Cy5 peaks and RhGr peaks are registered by the two detectors at the same time. This means that, at certain times, a very bright complex containing many RhGr-ONs and many Cy5-pLL chains moves through the excitation volume (16). The average fluorescence between the highly intense peaks (which we term “baseline fluorescence”) is significantly lower compared to free RhGr-ONs and free Cy5-pLL. This baseline fluorescence reflects the average number of free (i.e., noncomplexed) fluorescent molecules in the excitation volume. The decrease in baseline fluorescence is expected as the labeled ONs and carrier molecules organize into multimolecular complexes, thereby lowering the average number of free ONs and free polymer strands in the excitation volume. Upon adding dextran sulfate (an anionic polymer from which we know by gel electrophoresis that it is able to release the ONs from the complexes), the baseline fluorescence of RhGr-ONs is restored to its original value, and RhGr peaks do not occur anymore. From the fluorescence fluctuations a diffusion coefficient of $(0.77 \pm 0.06) \times 10^{-6}$ cm²/s was calculated, which corresponds to the diffusion coefficient of free RhGr-

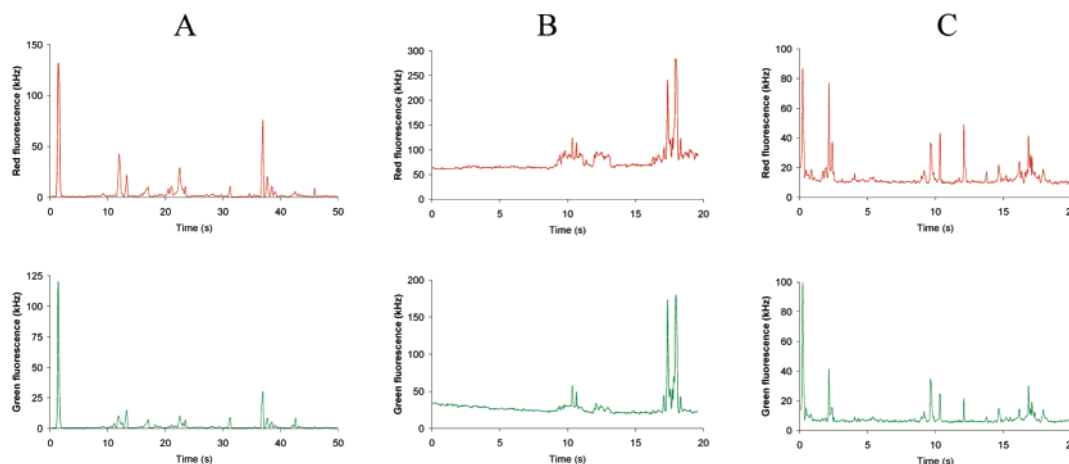


FIGURE 1: Fluorescence fluctuation profiles, as simultaneously registered by the red and green detector, of a dispersion of dual color labeled nanobeads (90 nm) in buffer (A), in the nucleus of a Vero cell after microinjecting the nucleus (B), and in the cytoplasm of a Vero cell after microinjecting the cytoplasm (C).

ONs [$(0.76 \pm 0.07) \times 10^{-6} \text{ cm}^2/\text{s}$] (16). This confirms that the RhGr-ONs were released from their carrier. However, the baseline fluorescence of Cy5-pLL is only partly restored, and the Cy5 peaks remained. We suggest that only part of the Cy5-pLL chains are released while part of them bind to dextran sulfate, resulting into highly red-fluorescent Cy5-pLL/dextran sulfate complexes.

FFS on Dual Color Labeled Nanobeads in Buffer and in Cells. As a control experiment, dual color FFS measurements were first performed in the cytoplasm and nucleus of “blanc” cells (i.e., cells which were not loaded with fluorescent molecules or fluorescent nanobeads). Generally, the fluorescence registered by the two detectors was very low while from time to time (very) small peaks appeared (the intensity of these peaks being maximally 3 kHz above the background noise).

To validate the applicability of FFS for studying the association state of complicated nanosized polymer/ON complexes in complex media such as the cytoplasm or the nucleus of cells, we first performed FFS measurements on dual-colored nanobeads (respectively 90 and 500 nm in diameter) injected in living cells. These dual-colored nanobeads are a positive control for intact dual-colored ON/polymer complexes. FFS measurements on a dispersion of these nanobeads in buffer revealed simultaneously occurring high fluorescence peaks of green and red fluorescence (Figure 1A). This clearly proves that the red and green detectors are indeed able to simultaneously detect a highly fluorescent, dual color labeled particle that migrates through the excitation volume.

We further performed FFS measurements on the nanobeads microinjected in Vero cells. Microinjecting 90 nm nanobeads in the nucleus (Figure 1B) or in the cytoplasm (Figure 1C) resulted in the simultaneous appearance of Cy5 and RhGr peaks in the detection volume (positioned at a different location than the site of injection). This proves that at least part of these beads are mobile in both the cytoplasm and nucleus. Microinjected 500 nm nanobeads seemed quasi-immobile in the cytoplasm as CLSM time-series experiments for 30 min did not reveal any diffusion of the beads (data not shown). Also, in FFS measurements, the microinjected 500 nm beads did not result into simultaneous RhGr peaks and Cy5 peaks, which we did see for these nanobeads in

buffer (data not shown), confirming that they were physically entrapped in the cytoplasm.

FFS on RhGr-ONs in Cells. Microinjection of free RhGr-ONs in the cytoplasm resulted in nuclear accumulation of the RhGr-ONs within minutes (CLSM images not shown). This rapid nuclear accumulation of ONs has also been reported in the literature (25–28). FFS measurements confirmed these observations as the RhGr baseline fluorescence was significantly higher in the nucleus than in the cytoplasm of the same cell: it varied between 60 to 200 kHz in the cytoplasm and between 150 and 600 kHz in the nucleus (dependent on the amount of RhGr-ONs injected, as according to the manufacturer no reproducible volume can be microinjected). In the fluorescence fluctuation profiles measured in the nucleus, RhGr peaks were absent (Figure 2A, upper profile), indicating that intensive clustering of the RhGr-ONs with nuclear components (which could result in highly green fluorescent structures) probably does not occur. Autocorrelation analysis of the fluorescence fluctuations revealed a significant slowing down of the RhGr-ONs (Figure 2B), which is in agreement with the recently demonstrated interaction between antisense ONs and their target mRNA in the nucleus (29). In the cytoplasm, however, RhGr peaks could be observed (Figure 2A, lower profile), indicating that RhGr-ONs are clustered with cytosolic components. Indeed, we recently observed that, after adding diluted cell lysate to labeled ONs, part of the ONs cluster together, which is observed as the appearance of high fluorescence peaks in the green fluorescence fluctuation profile (data not shown). The latter observation points out the need for a dual color FFS approach to study the dissociation of polymer/ON complexes in cells. Single color labeled aggregates could be due to nondissociated polymer/ON complexes (with the polymer *or* the ONs being labeled) but also to dissociated polymer/ON complexes whereby the polymer *or* the ONs subsequently cluster with cellular components. On the other hand, when dual color labeled aggregates are observed, they are certainly due to (nondissociated) polymer/ON complexes.

FFS on Cy5-Polymer/RhGr-ON Complexes in Cells. Microinjection of the cationic copolymer Cy5-graft-pDMAEMA in the cytoplasm resulted in a homogeneous distribution of the labeled polymer throughout the cytoplasm (data not shown). Clearly, the polymer did not reach the

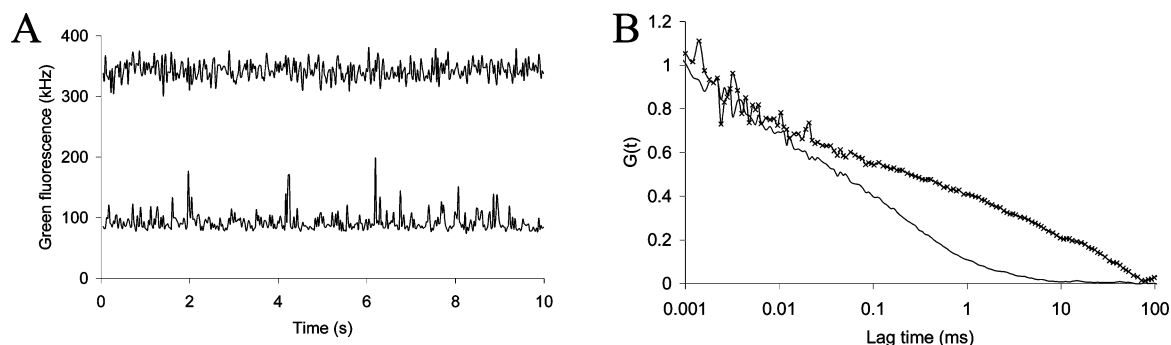


FIGURE 2: (A) Fluorescence fluctuations in the cytoplasm (lower profile) and in the nucleus (upper profile) of a Vero cell injected in the cytoplasm with RhGr-ONs. (B) Autocorrelation curve of RhGr-ONs in buffer (—) and in the nucleus of a Vero cell (—x—).

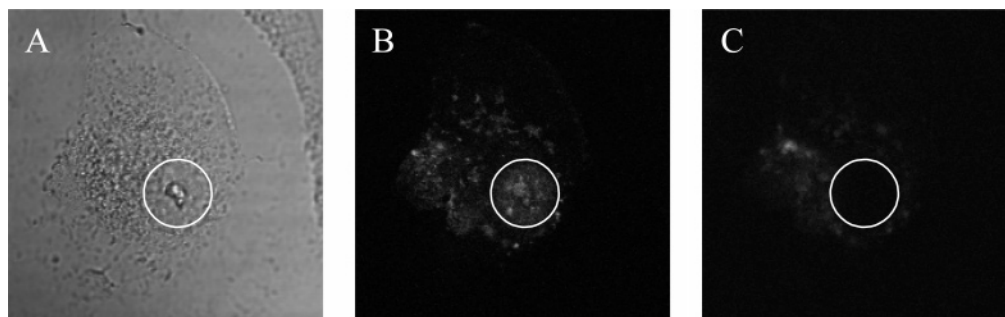


FIGURE 3: Transmission image (A) and confocal fluorescence images (B and C) of a Vero cell transfected for 3 h with Cy5-graft-pDMAEMA/RhGr-ONs. A circle is drawn around the nucleus.

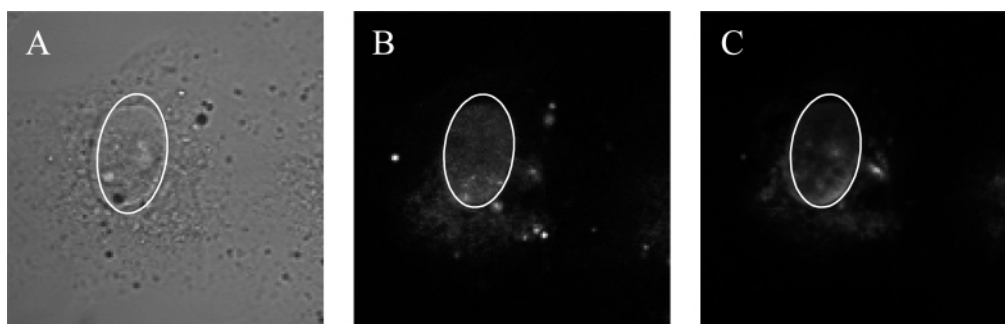


FIGURE 4: Transmission image (A) and confocal fluorescence images (B and C) of a Vero cell transfected for 3 h with Cy5-pLL/RhGr-ONs. An ellipse is drawn around the nucleus.

nucleus. It is well-known that only small structures can migrate passively through the nuclear pores (30). Therefore, it could well be expected that Cy5-graft-pDMAEMA of a molar mass of 1700 kDa would not be able to cross the nuclear membrane. After transfecting Vero cells with Cy5-graft-pDMAEMA/RhGr-ON complexes for 3 h, CLSM revealed that the polymer remained located in the cytoplasm whereas part of the oligonucleotides accumulated in the nucleus (and therefore must have been released from the polymer; Figure 3). Another part of the oligonucleotides remained present in the cytoplasm, predominantly colocalized with the polymer. This proves that Cy5-graft-pDMAEMA/RhGr-ON complexes, which are successfully taken up by the cells, are subsequently released from the endosomes and dissociate in the cytoplasm. This is in agreement with our previous results where graft-pDMAEMA proved to be an efficient carrier for antisense ONs. The biological activity could be observed when transfecting A549 cells with graft-pDMAEMA/ON complexes (31).

To conclude, CLSM experiments are sufficient to prove that (part of) the Cy5-graft-pDMAEMA/RhGr-ON complexes dissociate in the cytoplasm. When using a pharma-

ceutical carrier of lower molar mass, however, CLSM results may become insufficient to detect whether the complexes are associated or dissociated. Indeed, after incubating Vero cells with Cy5-pLL/RhGr-ONs for 3 h (the molar mass of pLL being 30 kDa), colocalized green and red spots were present in both the cytoplasm and the nuclei (Figure 4). However, this occurrence of colocalized green and red fluorescence in the cytoplasm and nuclei does not necessarily imply that all RhGr-ONs are still associated to their Cy5-pLL carrier. They may just be localized together without being associated. Via CLSM it is thus not possible to elucidate whether intact complexes were transported from the cytosol into the nucleus or whether dissociation occurred in the cytosol followed by nuclear accumulation of the free polymer and free ONs. Therefore, we thought that the temporal analysis of the movement of these molecules via FFS, instead of the spatial analysis of the fluorescent labeled molecules via CLSM, could be better to conclude whether the fluorescent labeled species are associated. Figure 5D shows that FFS is able to detect simultaneously occurring RhGr peaks and Cy5 peaks in the cytoplasm of Vero cells already after 30 min of incubation of the cells with Cy5-

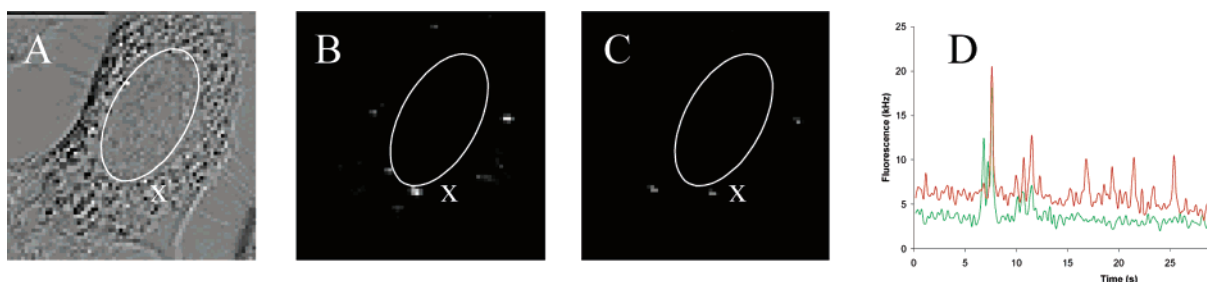


FIGURE 5: Transmission image (A) and confocal fluorescence images (B, green; C, red) of a Vero cell transfected for 30 min with Cy5-pLL/RhGr-ONs. An ellipse is drawn around the nucleus. The fluorescence fluctuation profile as registered by the green and red FFS detector when the excitation volume is positioned in the cell at location X (D).

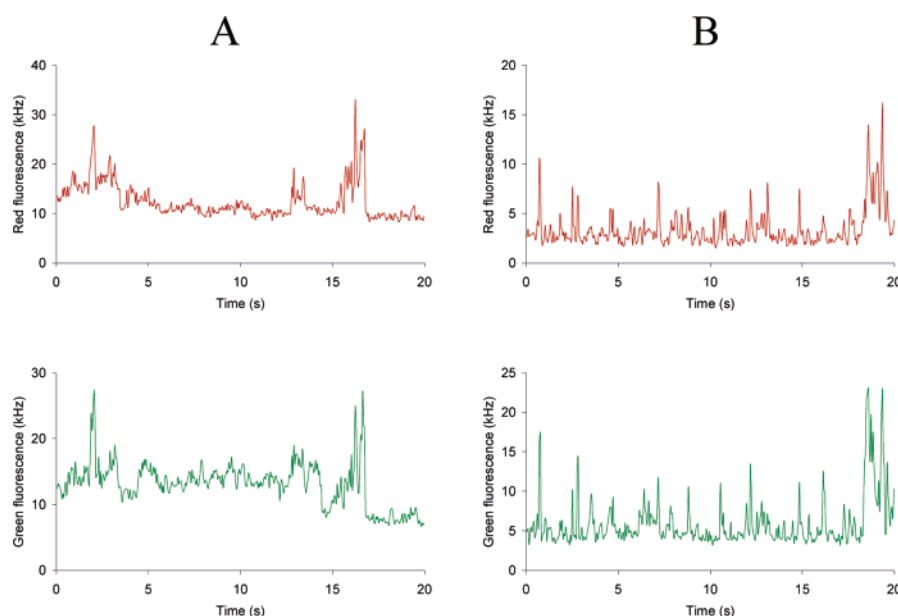


FIGURE 6: Fluorescence fluctuation profiles as registered by the green and red detector in the nucleus of a Vero cell after microinjecting the nucleus with a Cy5-pLL/RhGr-ON dispersion (A) and in the cytoplasm of a Vero cell after microinjecting the cytoplasm with a Cy5-pLL/RhGr-ON dispersion (B).

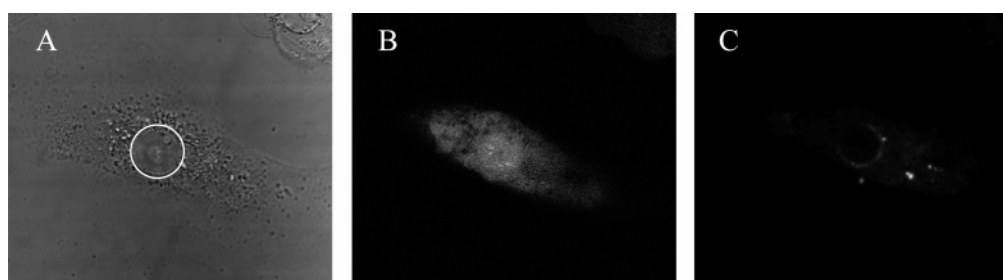


FIGURE 7: Transmission image (A) and confocal fluorescence images (B and C) of a Vero cell 15 min after injecting the cytoplasm with a dispersion which consists of Cy5-pLL/dextran sulfate complexes and released RhGr-ONs. A circle is drawn around the nucleus.

pLL/RhGr-ON complexes. This means that multimolecular Cy5-pLL/RhGr-ON complexes are able to diffuse through the cytoplasm and pass through the excitation volume. After longer incubation time, FFS was able to detect both Cy5-pLL and RhGr-ONs in the nucleus. However, simultaneously occurring Cy5 and RhGr peaks were never observed in the nucleus (data not shown). This indicates that Cy5-pLL and RhGr-ONs migrate independently from each other in the nucleus. On the other hand, it remains possible that intact polyplexes were present in the nucleus but that they were not detected by FFS as they did not migrate (or migrate too slowly) through the nuclear matrix and thus did not move through the excitation volume. To clarify this hypothesis we microinjected Cy5-pLL/RhGr-ON complexes into the nucleus

of Vero cells. The simultaneous appearance of RhGr peaks and Cy5 peaks in Figure 6A clearly indicates that Cy5-pLL/RhGr-ON complexes migrate through the excitation volume, proving that FFS is able to detect intact Cy5-pLL/RhGr-ON complexes in the nucleus. Therefore, from the absence of simultaneous peaks in the nuclei of the Cy5-pLL/RhGr-ON transfected cells, it can be concluded that intact polyplexes did not reach the nucleus. This means that the Cy5-pLL/RhGr-ON complexes first dissociate in the cytoplasm before the RhGr-ONs and the Cy5-pLL strands enter the nucleus. Such conclusion cannot be based upon CLSM experiments.

Also, other pharmaceutical carriers of low molar mass are reported to enter the nucleus after transfection (11, 32, 33). We also observed in our experiments that microinjection of

free Cy5-pLL resulted into nuclear accumulation. To further demonstrate the power of FFS to study the intracellular behavior of ON complexes, we dissociated Cy5-pLL/RhGr-ON complexes with dextran sulfate prior to their microinjection in the cytoplasm of a Vero cell. Figure 7 clearly shows that the free RhGr-ONs accumulate in the nucleus, whereas the Cy5-pLL, bound to the high molar mass dextran sulfate, is now unable to access the nucleus. Also, as expected, FFS measurements in the cytoplasm of this cell revealed Cy5 peaks, attributed to the Cy5-pLL/dextran sulfate complexes migrating through the excitation volume (data not shown).

CONCLUSIONS

We have shown that cationic polymers of *high* molar mass, like *graft*-pDMAEMA of 1700 kDa used in this study, cannot enter the nucleus after microinjection in the cytoplasm. When such (red-labeled) polymers are used as a carrier for (green-labeled) ONs, CLSM experiments are sufficiently suited to prove whether the polymer/oligonucleotide complexes are able to dissociate in the cytoplasm or not: after dissociation the released green-labeled ONs enter the nucleus while the red-labeled polymer chains remain in the cytoplasm; consequently, the red and green labels do not colocalize in the nucleus. However, contrary to the high molar mass cationic polymers, cationic polymers of *lower* molar mass, such as pLL of 30 kDa used in this study, do enter the nucleus upon microinjection or transfection. Consequently, when such (red-labeled) polymers are used as carriers for (green-labeled) ONs, the nuclei might show both green and red fluorescence, regardless of whether the polyplexes are dissociated or not. Clearly, CLSM experiments cannot reveal whether the dual-colored nuclei are due to intact Cy5-pLL/RhGr-ON polyplexes or to dissociated Cy5-pLL and RhGr-ON chains. Our results show that dual-colored FFS, which monitors the movement of the fluorescent molecules, can solve this question. After cytoplasmic microinjection or after transfection with Cy5-pLL/RhGr-ON complexes, FFS was able to detect simultaneously red and green fluorescence peaks in the cytoplasm. In the nucleus, however, simultaneous peaks were never observed. From these results we could conclude that the Cy5-pLL and RhGr-ONs present in the nucleus after transfection were not associated.

ACKNOWLEDGMENT

The authors appreciate the assistance and guidance of Dr. Rainer Pepperkok during the stay of Bart Lucas and Katrien Remaut at his laboratory (Cell Biology/Cell Biophysics Programm, EMBL Heidelberg, Germany). The contribution of Ine Lentacker in the execution of the practical work is acknowledged. *graft*-pDMAEMA was a kind gift of Prof. W. E. Hennink (University of Utrecht).

REFERENCES

- Stein, C. A., and Cheng, Y. C. (1993) Antisense oligonucleotides as therapeutic agents—Is the bullet really magical?, *Science* **261**, 1004–1012.
- Elbashir, S. M., Harborth, J., Lendeckel, W., Yalcin, A., Weber, K., and Tuschl, T. (2001) Duplexes of 21-nucleotide RNAs mediate RNA interference in cultured mammalian cells, *Nature* **411**, 494–498.
- Harborth, J., Elbashir, S. M., Vandeburgh, K., Manninga, H., Scaringe, S. A., Weber, K., and Tuschl, T. (2003) Sequence, chemical, and structural variation of small interfering RNAs and short hairpin RNAs and the effect on mammalian gene silencing, *Antisense Nucleic Acid Drug Dev.* **13**, 83–105.
- Miyagishi, M., Hayashi, M., and Taira, K. (2003) Comparison of the suppressive effects of antisense oligonucleotides and siRNAs directed against the same targets in mammalian cells, *Antisense Nucleic Acid Drug Dev.* **13**, 1–7.
- Filmore, D. (2004) Assessing antisense. An NDA withdrawal signals another setback, but hope remains for next-generation drugs, *Mod. Drug Discovery*, 49–50 (June).
- De Smedt, S. C., Demeester, J., and Hennink, W. E. (2000) Cationic polymer based gene delivery systems, *Pharm. Res.* **17**, 113–126.
- Gao, X., and Huang, L. (1995) Cationic liposome-mediated gene transfer, *Gene Ther.* **2**, 710–722.
- Felgner, P. L., Barenholz, Y., Behr, J. P., Cheng, S. H., Cullis, P., Huang, L., Jessee, J. A., Seymour, L., Szoka, F., Thierry, A. R., Wagner, E., and Wu, G. (1997) Nomenclature for synthetic gene delivery systems, *Hum. Gene Ther.* **8**, 511–512.
- Zabner, J., Fasbender, A. J., Moninger, T., Poellinger, K. A., and Welsh, M. J. (1995) Cellular and molecular barriers to gene transfer by a cationic lipid, *J. Biol. Chem.* **270**, 18997–19007.
- Simeoni, F., Morris, M. C., Heitz, F., and Divita, G. (2003) Insight into the mechanism of the peptide-based gene delivery system MPG: implications for delivery of siRNA into mammalian cells, *Nucleic Acids Res.* **31**, 2717–2724.
- Godbey, W. T., Wu, K. K., and Mikos, A. G. (1999) Tracking the intracellular path of poly(ethylenimine)/DNA complexes for gene delivery, *Proc. Natl. Acad. Sci. U.S.A.* **96**, 5177–5181.
- Marcusson, E. G., Bhat, B., Manoharan, M., Bennett, C. F., and Dean, N. M. (1998) Phosphorothioate oligodeoxyribonucleotides dissociate from cationic lipids before entering the nucleus, *Nucleic Acids Res.* **26**, 2016–2023.
- Zelphati, O., and Szoka, F. C. (1996) Mechanism of oligonucleotide release from cationic liposomes, *Proc. Natl. Acad. Sci. U.S.A.* **93**, 11493–11498.
- Schwille, P. (2001) Fluorescence correlation spectroscopy and its potential for intracellular applications, *Cell Biochem. Biophys.* **34**, 383–408.
- Schwille, P., MeyerAlmes, F. J., and Rigler, R. (1997) Dual-color fluorescence cross-correlation spectroscopy for multicomponent diffusional analysis in solution, *Biophys. J.* **72**, 1878–1886.
- Lucas, B., Van Rompaey, E., De Smedt, S. C., Demeester, J., and Van Oostveldt, P. (2002) Dual-color fluorescence fluctuation spectroscopy to study the complexation between poly-L-lysine and oligonucleotides, *Macromolecules* **35**, 8152–8160.
- Lucas, B., Remaut, K., Braeckmans, K., Hastraete, J., De Smedt, S. C., and Demeester, J. (2004) Studying pegylated DNA-complexes by dual color fluorescence correlation spectroscopy, *Macromolecules* **37**, 3832–3840.
- Van Rompaey, E., Sanders, N., De Smedt, S. C., Demeester, J., Van Craenenbroeck, E., and Engelborghs, Y. (2000) Complex formation between cationic polymethacrylates and oligonucleotides, *Macromolecules* **33**, 8280–8288.
- Van Rompaey, E., Engelborghs, Y., Sanders, N., De Smedt, S. C., and Demeester, J. (2001) Interactions between oligonucleotides and cationic polymers investigated by fluorescence correlation spectroscopy, *Pharm. Res.* **18**, 928–936.
- Van Rompaey, E., Chen, Y., Muller, J. D., Gratton, E., Van Craenenbroeck, E., Engelborghs, Y., De Smedt, S., and Demeester, J. (2001) Fluorescence fluctuation analysis for the study of interactions between oligonucleotides and polycationic polymers, *Biol. Chem.* **382**, 379–386.
- Snyder, S. L., and Sobocinski, P. Z. (1975) Improved 2,4,6-trinitrobenzenesulfonic acid method for determination of amines, *Anal. Biochem.* **64**, 284–288.
- Dijk-Wolthuis, W. N. E., van de Wetering, P., Hinrichs, W. L. J., Hofmeyer, L. J. F., Liskamp, R. M. J., Crommelin, D. J. A., and Hennink, W. E. (1999) A versatile method for the conjugation of proteins and peptides to poly[2-(dimethylamino)ethyl methacrylate], *Bioconjugate Chem.* **10**, 687–692.
- Schwille, P., MeyerAlmes, F. J., and Rigler, R. (1997) Dual-color fluorescence cross-correlation spectroscopy for multicomponent diffusional analysis in solution, *Biophys. J.* **72**, 1878–1886.
- Hess, S. T., Huang, S. H., Heikal, A. A., and Webb, W. W. (2002) Biological and chemical applications of fluorescence correlation spectroscopy: A review, *Biochemistry* **41**, 697–705.

25. Clarenc, J. P., Lebleu, B., and Leonetti, J. P. (1993) Characterization of the nuclear-binding sites of oligodeoxyribonucleotides and their analogs, *J. Biol. Chem.* 268, 5600–5604.
26. Hartig, R., Shoeman, R. L., Janetzko, A., Grub, S., and Traub, P. (1998) Active nuclear import of single-stranded oligonucleotides and their complexes with nonkaryophilic macromolecules, *Biol. Cell* 90, 407–426.
27. Lorenz, P., Baker, B. F., Bennett, C. F., and Spector, D. L. (1998) Phosphorothioate antisense oligonucleotides induce the formation of nuclear bodies, *Mol. Biol. Cell* 9, 1007–1023.
28. Tsuji, A., Koshimoto, H., Sato, Y., Hirano, M., Sei-Iida, Y., Kondo, S., and Ishibashi, K. (2000) Direct observation of specific messenger RNA in a single living cell under a fluorescence microscope, *Biophys. J.* 78, 3260–3274.
29. Shi, F. X., Visser, W. H., de Jong, N. M. J., Liem, R. S. B., Ronken, E., and Hoekstra, D. (2003) Antisense oligonucleotides reach mRNA targets via the RNA matrix: downregulation of the 5-HT1A receptor, *Exp. Cell Res.* 291, 313–325.
30. Liu, G., Li, D. S., Pasumathy, M. K., Kowalczyk, T. H., Gedeon, C. R., Hyatt, S. L., Payne, J. M., Miller, T. J., Brunovskis, P., Fink, T. L., Muhammad, O., Moen, R. C., Hanson, R. W., and Cooper, M. J. (2003) Nanoparticles of compacted DNA transfect postmitotic cells, *J. Biol. Chem.* 278, 32578–32586.
31. Lucas, B., Van Rompaey, E., Remaut, K., Sanders, N., De Smedt, S. C., and Demeester, J. (2004) On the biological activity of anti-ICAM-1 oligonucleotides complexed to nonviral carriers, *J. Controlled Release* 96, 207–219.
32. Clamme, J. P., Krishnamoorthy, G., and Mély, Y. (2003) Intracellular dynamics of the gene delivery vehicle polyethylenimine during transfection: investigation by two-photon fluorescence correlation spectroscopy, *Biochim. Biophys. Acta* 1617, 52–61.
33. Jensen, K. D., Nori, A., Tijerina, M., Kopeckova, P., and Kopecek, J. (2003) Cytoplasmic delivery and nuclear targeting of synthetic macromolecules, *J. Controlled Release* 87, 89–105.

BI0476883